IRRECOVERABLE AND RECOVERABLE NONLINEAR VISCOELASTIC PROPERTIES OF ASPHALT CONCRETE

James S. Lai, University of Utah; and
Douglas Anderson, Utah State Department of Highways

The results are reported of a series of uniaxial compression creep tests of an asphalt mixture under constant loadings, multiple-step loadings, and repeated loadings of as many as 100 cycles. It has been shown that the nonlinear viscoelastic behavior of the asphalt concrete can be represented by a nonlinear generalized Kelvin model that consists of a nonlinear dashpot connected in series with a nonlinear Kelvin chain. Thus, the nonlinear creep strains are separated into irrecoverable and recoverable strains. It has been shown that the constitutive equation can be determined by the use of both the creep and the recovery parts of the constant loading creep test results. The accuracy in predicting the creep behavior of the asphalt concrete under the multiple-step loadings and the repeated loadings has been shown to be very satisfactory. The importance of the irrecoverable strains to the practical implementation of asphalt pavements subjected to traffic loading is discussed. A possible way of relating the irrecoverable strains to the fatigue life of the material is also discussed.

•IN the past 10 years, considerable interest has been developed in an attempt to characterize the time and temperature dependence of the mechanical properties of asphalt paving mixtures within the framework of viscoelastic theory, especially the linear viscoelastic theory. Most of the test results reported so far on the viscoelastic characterization of asphalt mixtures have been obtained from the constant stress creep tests, or constant strain relaxation tests (1-4), and the sinusoidal loading tests (5-8). In most cases, the linear viscoelastic behavior of the asphalt concrete was assumed, and, henceforth, the linear viscoelastic material properties in terms of creep compliance, relaxation modulus, and complex compliance and complex modulus were obtained. For example, the phenomenon of creep can be represented by the following equation under a uniaxial stress state:

$$\epsilon(t) = \int_0^t J(t - \xi) \frac{\partial \sigma(\xi)}{\partial \xi} d\xi \qquad (1)$$

where ϵ and σ are uniaxial strain and stress respectively. J(t) is the uniaxial creep compliance and is usually determined from constant stress creep tests. For a given constant stress, Eq. 1 becomes

$$\epsilon(t) = J(t)\sigma_0 \quad \text{or} \quad J(t) = \frac{\epsilon(t)}{\sigma_0} \qquad (2)$$

In this equation, $\epsilon(t)$ is the measured creep strain under the constant stress σ_0, and the creep compliance J(t) can be obtained according to Eq. 2. In principle, if a material

Publication of this paper sponsored by Committee on Mechanical Properties of Bituminous Paving Mixtures.

is truly linearly viscoelastic, Eq. 1 with J(t) determined from Eq. 2 can be used to predict the creep behavior of the material under any kind of uniaxial loading history. However, this is not always true when the material is subjected to a more complex loading history.

In this report, the time-dependent properties of asphalt concrete are investigated under multiple-step loading histories, including several cyclic loading histories, in an effort to verify the applicability of linear viscoelastic theory in predicting the creep behavior under multiple-step loadings and also to construct a workable constitutive equation to describe more closely the time-dependent behavior of asphalt concrete under time-dependent loading histories.

In this report, the emphasis is also placed on distinction between the recoverable and irrecoverable creep under loading. This is important from a practical viewpoint because the irrecoverable creep strain contributes a large portion of the creep strain of asphalt concrete under external loading, and the irrecoverable strain is accumulative under repeated loading, whereas the recoverable creep is not necessarily.

MATERIALS AND SPECIMENS

A single asphalt mixture was utilized for the investigations. The asphalt cement used in preparing test specimens was from the American Oil Co. with 85 to 100 penetration grade. The asphalt content was 9 percent by weight. The gradation of aggregates is shown as follows:

Sieve Size	Percentage Passing
3/8 in.	100
No. 4	95.0
No. 8	60.0
No. 16	33.0
No. 50	15.0
No. 200	6.0

The test specimens used in this study were made of compressed asphalt concrete cylinders 2-in. in diameter and 3-in. in length. The asphalt mixture was pressed in a 2-in. diameter mold at 3,000 psi for 5 min at a temperature of 220 F. The specimens were cured in an oven at 140 F for 72 hours prior to the testing. Also, the randomness of the strain response of each specimen was minimized by subjecting each specimen to a 50-psi prestress for 12 min.

EXPERIMENTAL APPARATUS PROCEDURES

The basic test equipment shown in Figure 1 consists of a rigid frame A, a loading head B, a 1-to-10 ratio loading lever C, and the deformation measuring devices. A linear variable differential transducer (LVDT) was used to measure the deformation of the specimen. The output from LVDT, which is directly related to the total deformation, could be automatically recorded on a strip-chart recorder.

During the test, the specimen was placed directly under the loading head, and the LVDT was properly set. A selected dead weight was then put on the loading lever to produce a constant load on the specimen. The temperature during the test was kept at 75 ±2 F.

RESULTS AND ANALYSIS

Nine tests at three stress levels (10, 30, and 50 psi) were performed on prestressed samples. Duration of the loading period varied from 10 to 1,000 sec (i.e., 10, 100, and 1,000 sec). The results of the constant stress creep tests at three stress levels at three loading periods are shown in Figures 2, 3, and 4. Each solid line is the average of several repeated test results. In these figures, the recovery strains following each creep test are also shown.

Using Eq. 2, we can obtain the creep compliance J(t) as follows. Once the creep

Figure 1. Basic equipment for unconfined compressive creep test.

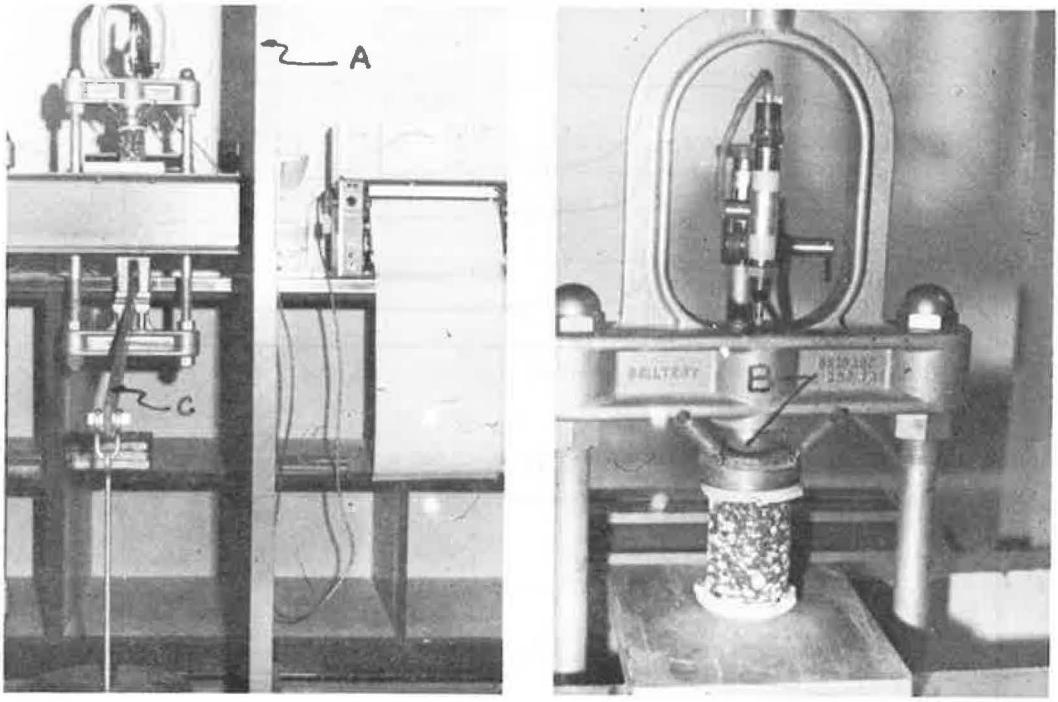

Figure 2. Creep and recovery of constant stress creep tests (t_i = 10 sec).

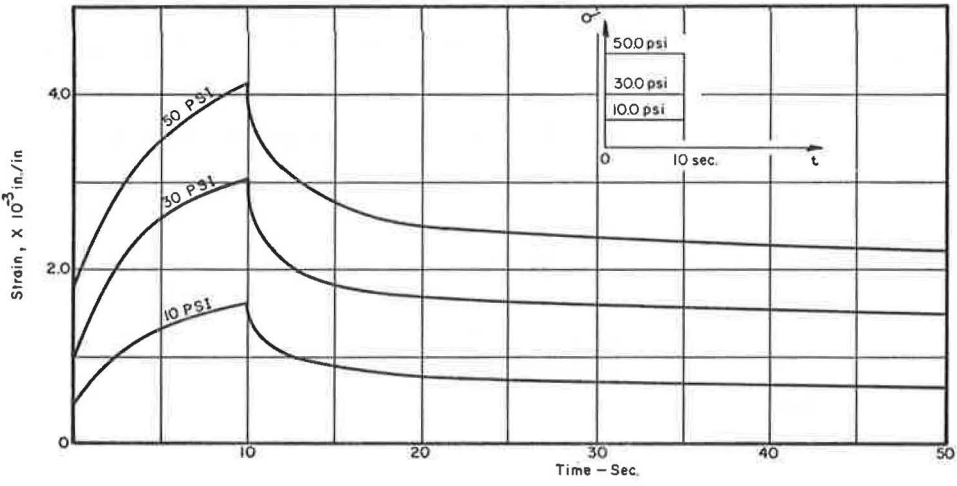

Figure 3. Creep and recovery of constant stress creep tests (t_i = 100 sec).

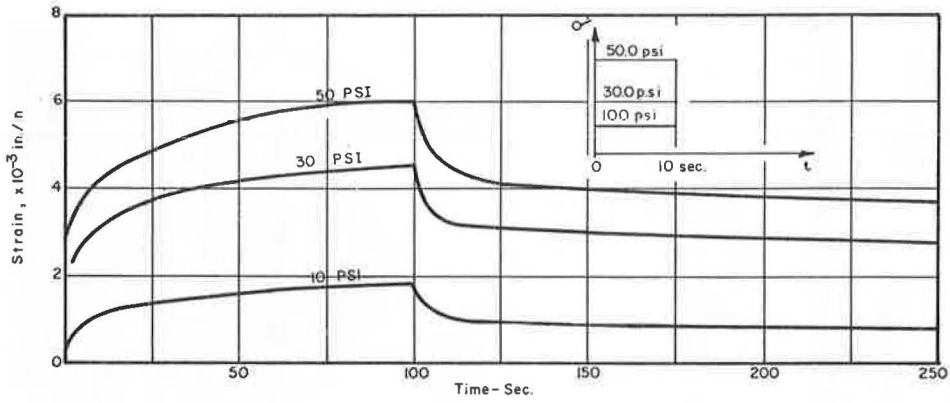

Figure 4. Creep and recovery of constant stress creep tests (t_i = 1,000 sec).

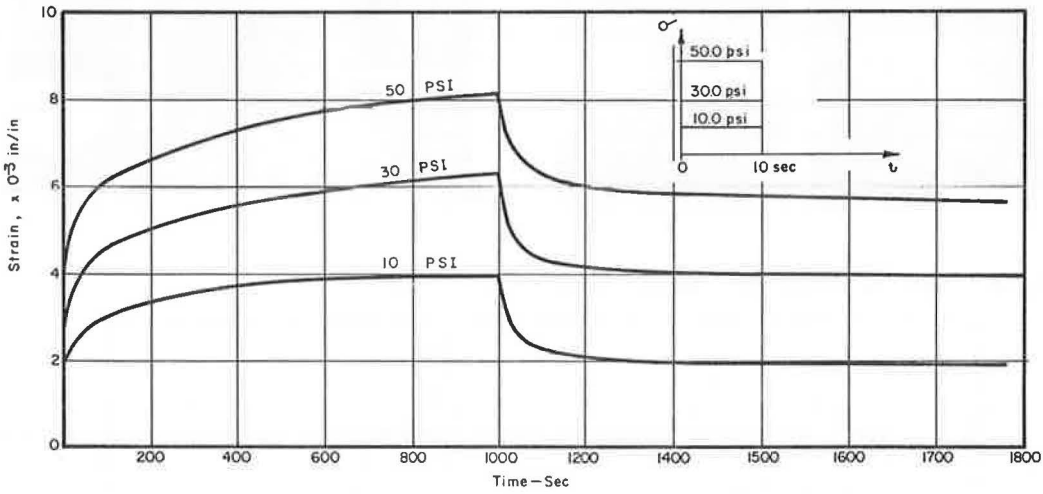

Figure 5. Constant stress creep curves plotted in log-log scale.

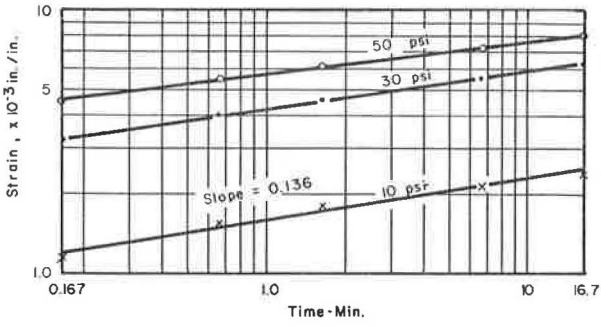

curves on the log-strain versus log-time base were replotted, they appeared to be straight lines as shown in Figure 5. Because the straight lines at three stress levels (Fig. 5) have nearly the same slope (0.136), the creep behavior could be expressed in the following form:

$$\epsilon_T(t) = A_T t^{n_T} \tag{3}$$

where ϵ_T is the total creep strain, and A_T is the strain at unit time (t = 1 min). The fact that A_T varies with stress can be seen by cross-plotting the strain values at t = 1 min of Figure 5 and the stress as shown in Figure 6 (open circles) and can be represented by the following relation:

$$\left.\begin{aligned} \epsilon_T(t) &= A_T(\sigma)t^{n_T} \\ A_T(\sigma) &= a_1\sigma + a_2\sigma^2 \\ a_1 &= 0.159 \times 10^{-3} \\ a_2 &= -0.857 \times 10^{-6} \end{aligned}\right\} \tag{4}$$

The creep compliance J(t), which is defined as $\frac{\epsilon(t)}{\sigma_0}$, can be obtained from Eq. 4 as follows:

$$J(t) = (a_1 + a_2\sigma)\, t^{n_T} \tag{5}$$

In view of Eq. 4 or 5, the asphalt concrete exhibits nonlinear behavior. Although a more popular form of power-law representation, such as σ^n, can be used as accurately as Eq. 4 to represent the stress dependence of A_T, this type of representation violates the basic invariance requirements as imposed from the continuum mechanics standpoint. Furthermore, Eq. 4 can be extended readily to represent the creep behavior under multiple stress states (11), whereas the power-law representation cannot.

Because the asphalt concrete was found to be nonlinear from the constant stress creep test, the second linearity requirement, the linear superposition principle, is not applicable any more. However, the modified superposition method (9-13) has been used to describe the nonlinear creep behavior and has been shown to be applicable in describing the creep behavior under arbitrary loading from the constant stress creep test results of many nonlinear viscoelastic materials. This modified superposition method is employed here to describe the recovery behavior. The modified superposition method yields the following form (9) for the recovery after constant stress creep:

$$\epsilon_r(t) = \epsilon[\sigma(t)] - \epsilon[\sigma(t - t_1)] \qquad t > t_1 \tag{6}$$

where $\epsilon[\sigma(t)]$ represents the creep strain under constant stress input, such as Eq. 4, and t_1 the unloading time. Inserting Eq. 4 into Eq. 6 yields

$$\epsilon_r(t) = (a_1\sigma + a_2\sigma^2)\left[t^{n_T} - (t - t_1)^{n_T}\right] \tag{7}$$

For n_T less than 1, as shown in Eq. 4 for the asphalt concrete, Eq. 7 predicts that the recovery strain approaches zero. The recovery curves shown in Figures 2, 3, and 4 indicate, however, a large irrecoverable strain (permanent set). Apparently Eq. 7 is not capable of describing the recovery behavior because either the modified superposition principle is not applicable for this material or Eq. 4, determined from the constant stress creep test results, does not represent the actual constitutive relation of the material. Therefore, an attempt was made using both the creep curves and the recovery curves of Figures 2, 3, and 4 to obtain a better representation of the constitutive relation of the material.

Because of the large portion of the unrecoverable strain of each creep test and because the amount of unrecoverable strain is dependent on the length of the loading period,

Figure 6. Creep strain-stress at unit time.

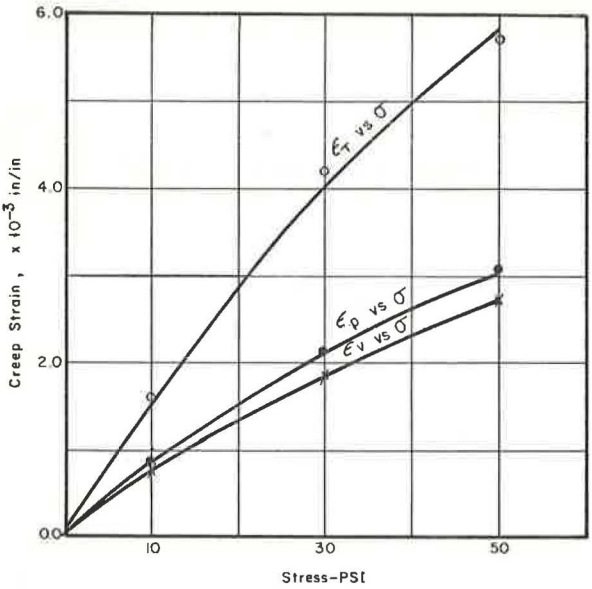

Figure 7. Nonlinear generalized Kelvin model.

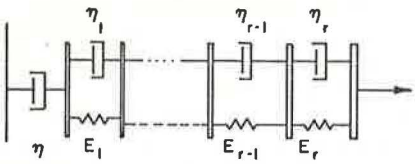

Figure 8. Irrecoverable strain versus time.

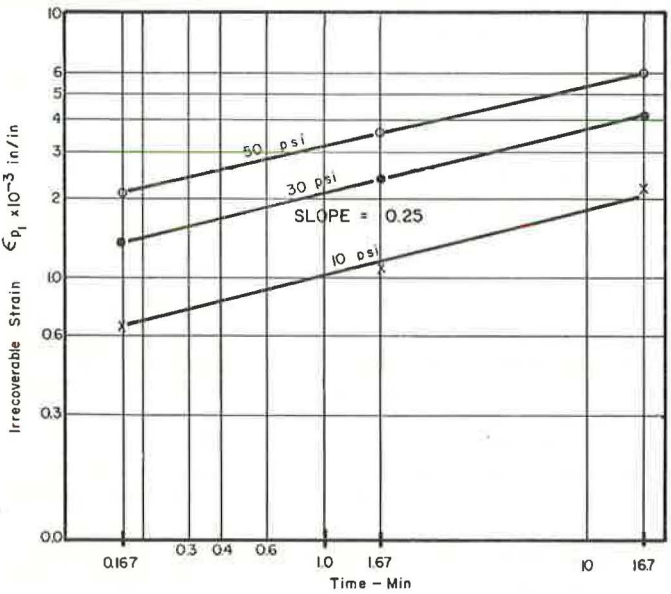

the creep behavior may be represented by a generalized nonlinear Kelvin model as shown in Figure 7. Here, the nonlinear dashpot may contribute to the irrecoverable strain, and the series of Kelvin models (Kelvin chain) may contribute to the power-law creep behavior (11). Therefore, the total creep strains (ϵ_T) of each test were separated into two parts, the irrecoverable strains (ϵ_p) due to the nonlinear dashpot and the completely recoverable strains (ϵ_v) due to the nonlinear Kelvin chain. The irrecoverable strains versus the length of the loading period (10, 100, and 1,000 sec) at each stress level on a log-log scale were plotted to form three straight lines as shown in Figure 8. Because these three straight lines have nearly the same slope of 0.25, the following expression can be obtained for irrecoverable strains:

$$\epsilon_p(t) = A_p t^{n_P} \tag{8}$$

Again, by cross-plotting the ϵ_p at t = 1.0 min and the stress as shown in Figure 6 (closed circles) and using the stress polynomial to fit those points, we can obtain the following equation:

$$\left.\begin{aligned} \epsilon_p(t) &= (b_1\sigma + b_2\sigma^2)\, t^{n_P} \\ b_1 &= 0.0844 \times 10^{-3} \\ b_2 &= -0.454 \times 10^{-6} \\ n_p &= 0.25 \end{aligned}\right\} \tag{9}$$

The rate of the irrecoverable strain $\dot{\epsilon}_p$ can be obtained from Eq. 9 as follows:

$$\dot{\epsilon}_p(t) = n_p(b_1\sigma + b_2\sigma^2)\, t^{n_P-1} \tag{10}$$

Instead of using Eq. 10, it was found that the "strain hardening theory" that relates the rate of the irrecoverable strain to the current stress and irrecoverable strain yielded a better description of the irrecoverable strain. The rate of the irrecoverable strain can be obtained by eliminating the time variable from Eqs. 7 and 10, which yields

$$\dot{\epsilon}_p(t) = n_p(b_1\sigma + b_2\sigma^2)^{1/n_P} \epsilon^{(n_P-1)/n_P} \tag{11}$$

or

$$\dot{\epsilon}_p(t) = \eta(\sigma, \epsilon_p)\sigma \tag{12}$$

$$\eta(\sigma, \epsilon_p) = n_p\left[\frac{1}{\sigma}(b_1\sigma + b_2\sigma^2)^{1/n_P}\right]\epsilon_p^{(n_P-1)/n_P} \tag{12a}$$

Equations 12 and 12a show that the dashpot is nonlinear and that the "coefficient of viscosity" η is dependent on the stress and the irrecoverable strain.

The recoverable strains ϵ_v due to the Kelvin chain were then obtained by subtracting the irrecoverable strains ϵ_p from the total strains ϵ_T. Thus, the total creep strains were separated into the recoverable part and the irrecoverable part.

Again, by using the same technique of plotting the ϵ_v versus time in the log-log scale, as shown in Figure 9, and cross-plotting in Figure 6, we can express the recoverable strains in the following form:

$$\left.\begin{aligned} \epsilon_v(t) &= (C_1\sigma + C_2\sigma^2)\, t^{n_v} \\ C_1 &= 0.0748 \times 10^{-3} \\ C_2 &= -0.412 \times 10^{-6} \\ n_v &= 0.093 \end{aligned}\right\} \tag{13}$$

The constitutive relation for the asphalt concrete using the generalized Kelvin model is summarized as follows for the constant stress creep:

$$\epsilon_T(t) = \epsilon_p(t) + \epsilon_v(t) \tag{14}$$

where ϵ_p is given by Eq. 12, and ϵ_v is given by Eq. 13. For the time-dependent stress input, the following equation is utilized:

$$\epsilon_T(t) = \int_0^t \dot{\epsilon}_p(\xi)d\xi + \int_0^t (t - \xi)^{n_v} [C_1 + 2C_2\sigma(\xi)]\ \dot{\sigma}(\xi)d\xi \tag{15}$$

In Eq. 15, the modified superposition method was again used (in the second integral) to describe the recoverable part of the creep strains under time-dependent stress input (10, 11, 12).

RESULTS AND PREDICTION OF CREEP UNDER MULTIPLE-STEP LOADING

In order to test and improve the application of Eq. 15 to the creep behavior of the asphalt concrete, we performed four multiple-step loading creep tests. The results are shown in Figures 10 through 13.

Equations 12, 13, and 15 were utilized to predict the creep behavior under multiple-step loading as follows. The stress inputs of the multiple steps can be expressed in a single algebraic equation using the Heaviside's unit function

$$\sigma(t) = \sum_{i=0}^{n} (\sigma_i - \sigma_{i-1})\ H(t - t_i) \tag{15a}$$

where $H(t - t_i)$ is the Heaviside's unit function, which has the value of 1 when $t \geq t_i$, 0 when $t < 0$, $\sigma_{-1} = 0$, and $t_0 = 0$. Inserting Eq. 15a into Eq. 15, after performing the integration, yields the following for the total strain at each loading step where

$$\epsilon_T(t) = \epsilon_p(t) + \epsilon_v(t) \tag{16}$$

For $0 < t < t_1$,

$$\epsilon_p(t) = [(b_1\sigma_0 + b_2\sigma_0^2)^{1/n_P} t]^{n_P} \tag{17a}$$

$$\epsilon_v(t) = (C_1\sigma_0 + C_2\sigma_0^2)\ t^{n_v} \tag{17b}$$

For $t_1 < t < t_2$,

$$\epsilon_p(t) = [(b_1\sigma_0 + b_2\sigma_0^2)^{1/n_P} t_1 + (b_1\sigma_1 + b_2\sigma_1^2)^{1/n_P}(t - t_1)]^{n_P} \tag{18a}$$

$$\epsilon_v(t) = (C_1\sigma_0 + C_2\sigma_0^2)\ [t^{n_v} - (t - t_1)^{n_v}] + (C_1\sigma_1 + C_2\sigma_1^2)\ (t - t_1)^{n_v} \tag{18b}$$

For $t_{r-1} < t < t_r$, $r = 1, 2, 3, \ldots$,

$$\epsilon_p(t) = [(b_1\sigma_0 + b_2\sigma_0^2)^{1/n_P}\ t_1 + \ldots\ (b_1\sigma_{r-2} + b_2\sigma_{r-2}^2)^{1/n_P}\ (t_{r-1} - t_{r-2}) + (b_1\sigma_{r-1} + b_2\sigma_{r-1}^2)^{1/n_P}(t - t_{r-1})]^{n_P} \tag{19a}$$

Figure 9. Recoverable strain versus time.

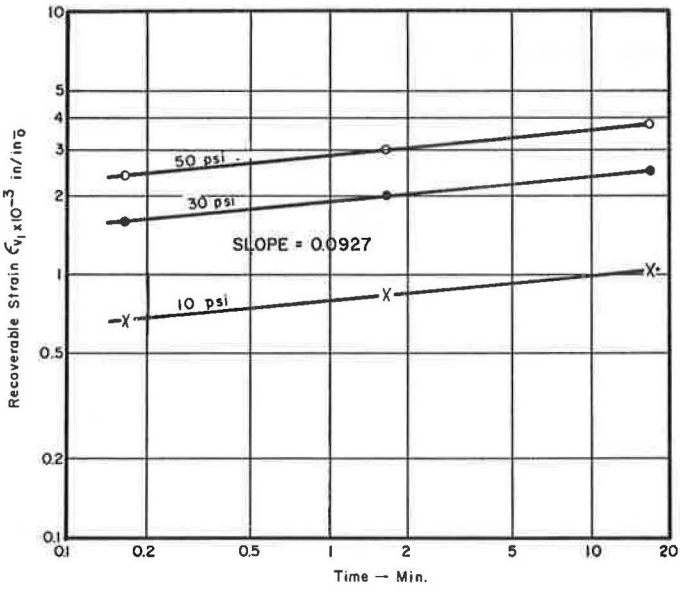

Figure 10. Results and predictions of creep behavior under step loading.

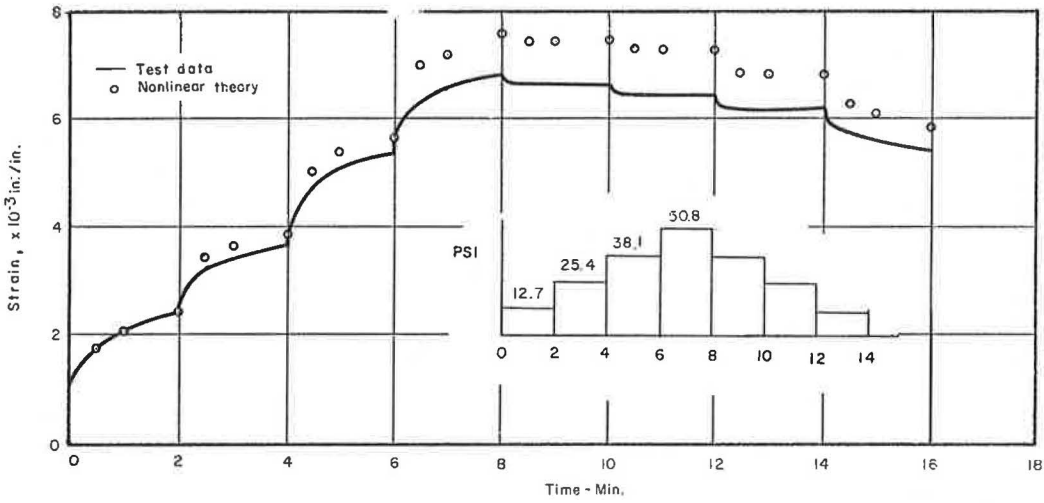

Figure 11. Results and predictions of creep behavior under step loading.

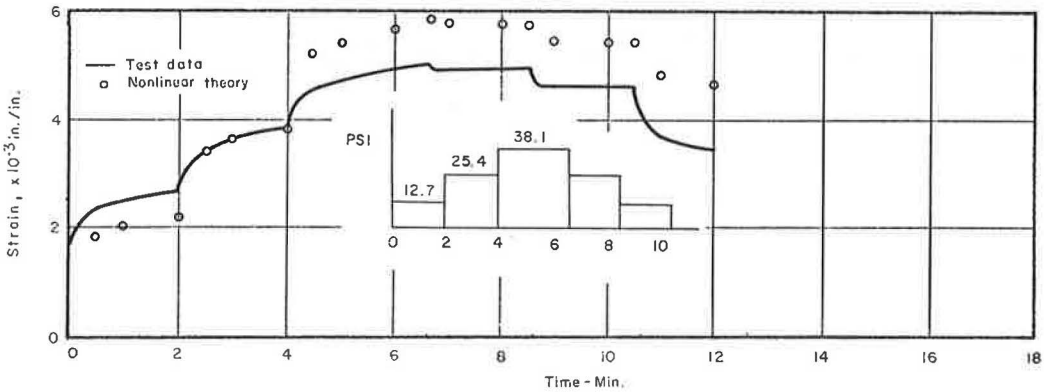

Figure 12. Results and predictions of creep behavior under step loading.

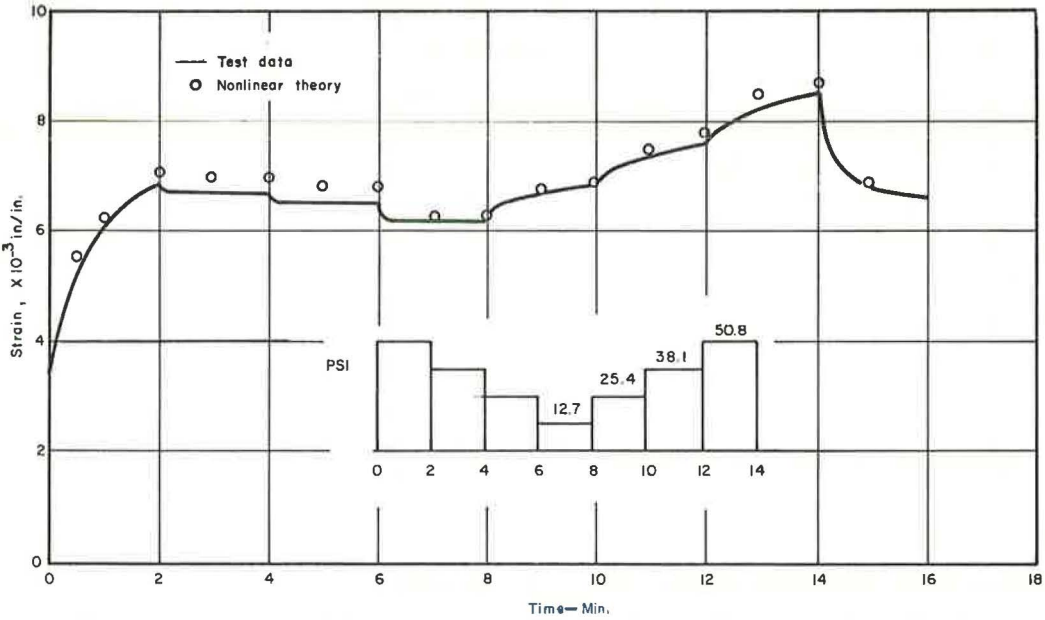

Figure 13. Results and predictions of creep behavior under step loading.

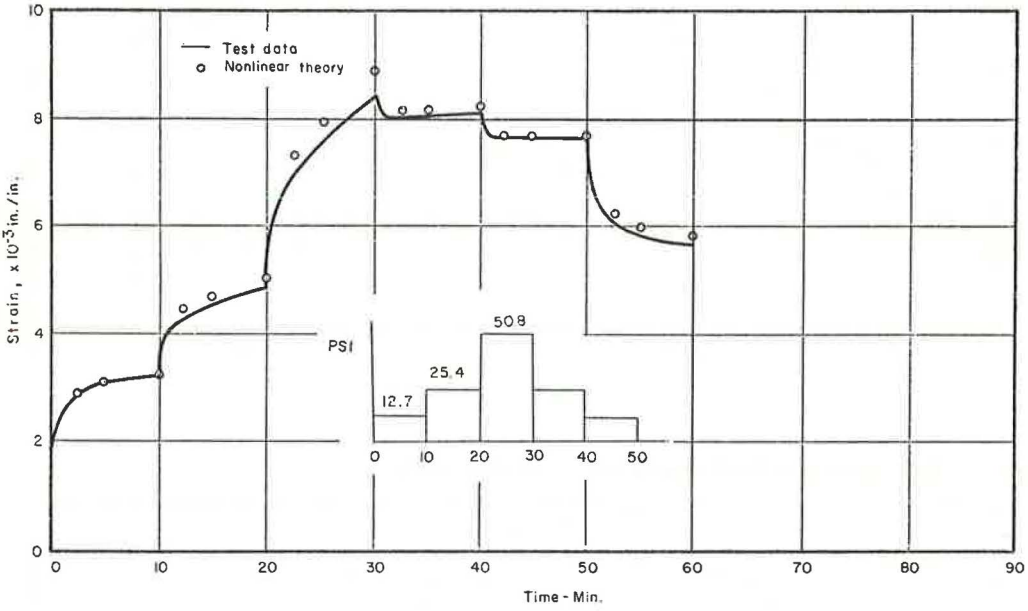

$$\epsilon_v(t) = (C_1\sigma_0 + C_2\sigma_0^2)\,[t^{n_v} - (t - t_1)^{n_v}] + \ldots$$
$$+ (C_1\sigma_{r-2} + C_2\sigma_{r-2}^2)\,[(t - t_{r-2})^{n_v} - (t - t_{r-1})^{n_v}]$$
$$+ (C_1\sigma_{r-1} + C_2\sigma_{r-1}^2)\,(t - t_{r-1})^{n_v} \qquad (19b)$$

By adding the predicted irrecoverable strains ϵ_p and the predicted recoverable strains ϵ_v, the predicted total creep strains ϵ_T under multiple-step loading can be obtained and are shown as the open circles in Figures 10 through 13 together with the experimental results that are depicted by the solid lines. The overall comparisons are quite satisfactory.

RESULTS AND PREDICTION OF CREEP UNDER REPEATED LOADING

The theory for a loading-unloading type of input was tested by loading specimens for 1 min and allowing them to recover in an unloaded state for 3 min before reloading. Cycles of this type were applied to specimens of 10, 20, 30, 40, and 50 psi, up to eight cycles. In addition, a 40-psi, 100-cycle repeated test was also conducted. The results are shown in Figures 14 through 19.

Again, using Eqs. 15, 19a, and 19b, the creep strains under the repeated loading were calculated as shown in Figures 14 through 18 for the eight-cycle tests. The theory predicts well for both the loading period and the unloading period of each cycle, though more deviation was observed in the recovery period.

These periodic loading tests are particularly important in the evaluation of asphalt concrete because pavements are constantly subjected to a similar loading pattern. Traffic passing over the pavement creates a loading period that is followed by an unloaded period. The loading time and stress are of primary importance to the total creep strain; thus, heavier, slower moving traffic causes greater "permanent" deformation. Although the total strain (or the shape of the total creep strain output with each loading cycle) is interesting and in many ways useful, the main concern when dealing with this type of material and stress pattern must lie not with the recoverable portion but with the irrecoverable strain introduced with each cycle. It can be seen from Figures 20 and 21 that the irrecoverable portion causes the accumulation of the total strain. Therefore, when the material is subjected to a large number of cyclic loadings, it may seem justified to deal mainly with expressions for the irrecoverable strain and to neglect the recoverable strain. In Figure 20, the theoretical and the experimental total strains and the irrecoverable strains at the end of each loading cycle were plotted against the number of cycles. The difference between total strain and the irrecoverable strain, which equals the recoverable, is small in comparison with the total strain or the irrecoverable strain. This figure also points out the range in which the theory is applicable. The increase in strain for each cycle remains fairly constant up to approximately 60 cycles. At this point, the rate begins to increase, and more deformation is observed with each cycle than in the previous cycle as shown in Figures 19 and 20. This is also where the theory and the observed strains begin to differ, leading to the conclusion that the equations predict the output within about 2.2 percent strain in this case, which is reached at about 60 cycles. A significant change in the shape of the specimen was also observed at about 60 cycles. The sample began to take on a barrel shape, increasing the cross-sectional area and most likely weakening a great deal of the internal bonds. In the region lower than 2.2 percent strain, where the increase in total deformation from one cycle to the next remains nearly constant, the cycles are very uniform in shape. Both the loading and recovery periods, after the first few cycles, demonstrate constant strain rates and magnitudes.

By letting N be the cycle number, Δt be the duration of the loading period of each cycle, and σ_0 be the constant stress at the load period, Eq. 19a becomes

$$\epsilon_p = (b_1\sigma_0 + b_2\sigma_0^2)\,[N(\Delta t)]^{n_p} \qquad (20)$$

where ϵ_p represents the irrecoverable strains at the end of the Nth loading cycle. The parameters contribute to the buildup of the irrecoverable strain, which is shown in

Figure 14. Results and predictions of creep behavior under cyclic loading (10-psi stress amplitude).

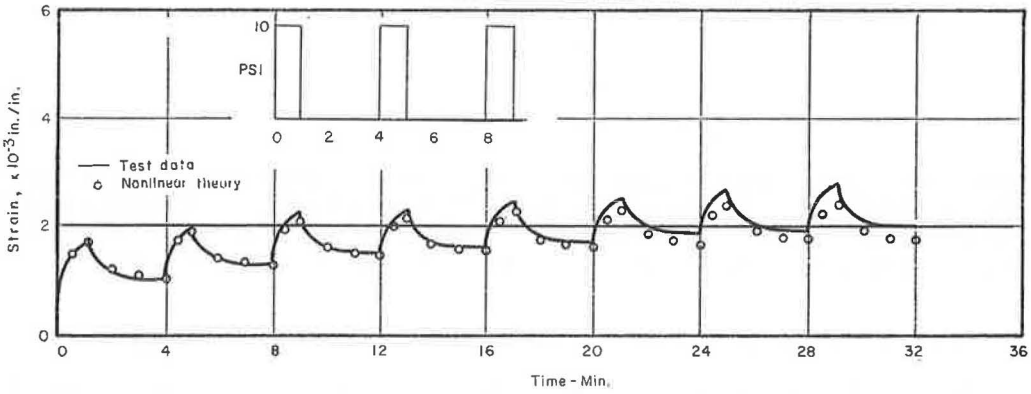

Figure 15. Results and predictions of creep behavior under cyclic loading (20-psi stress amplitude).

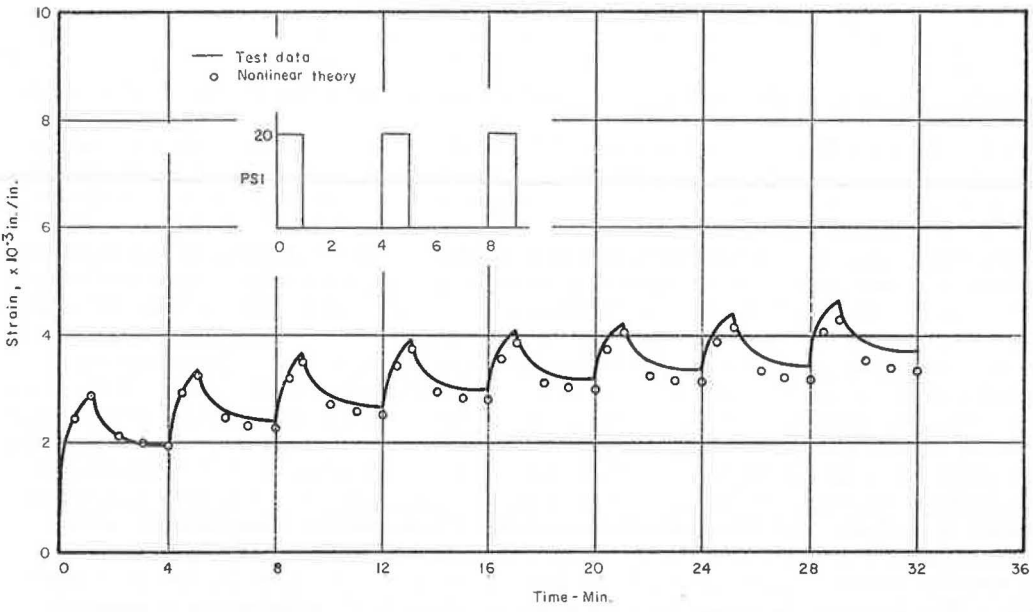

Figure 16. Results and predictions of creep behavior under cyclic loading (30-psi stress amplitude).

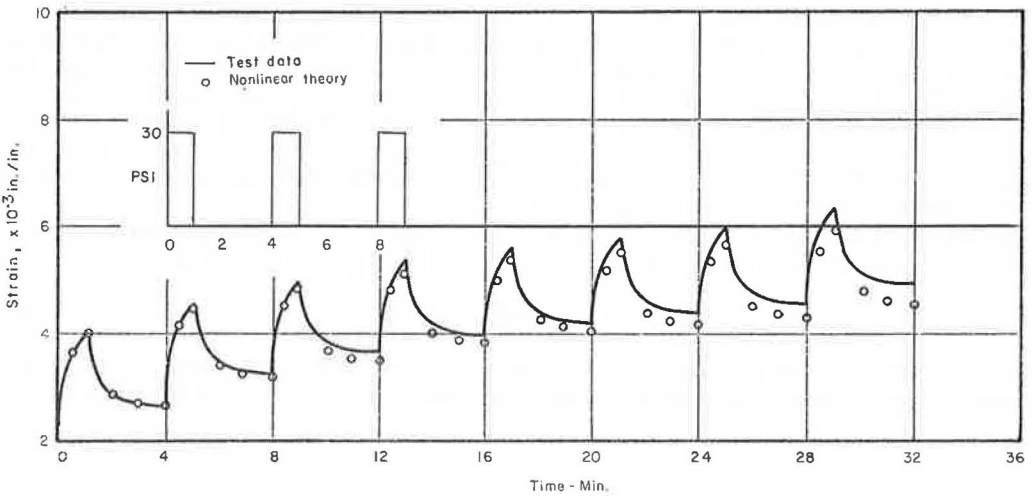

Figure 17. Results and predictions of creep behavior under cyclic loading (40-psi stress amplitude).

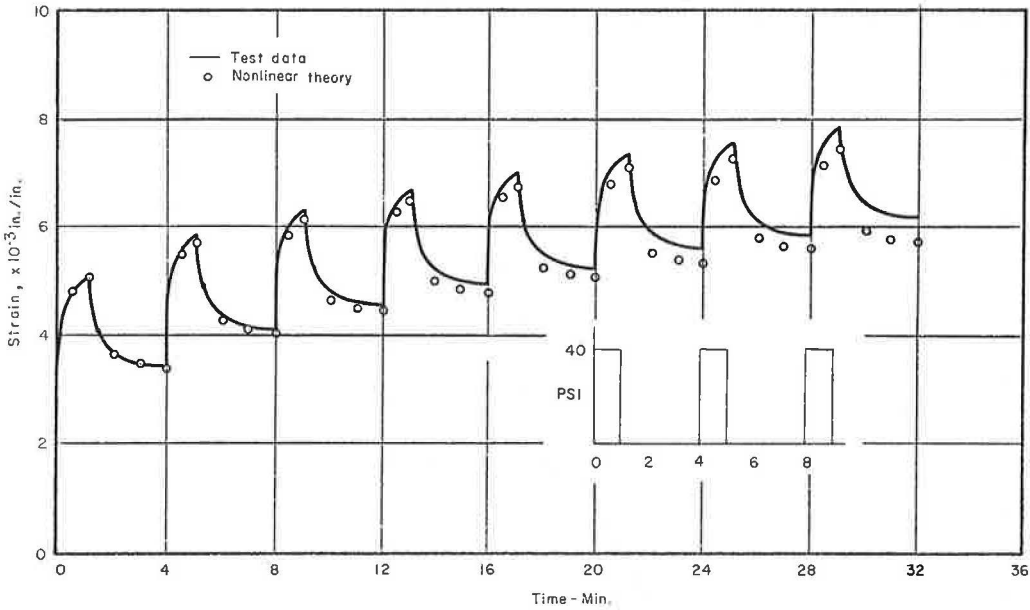

Figure 18. Results and predictions of creep behavior under cyclic loading (50-psi stress amplitude).

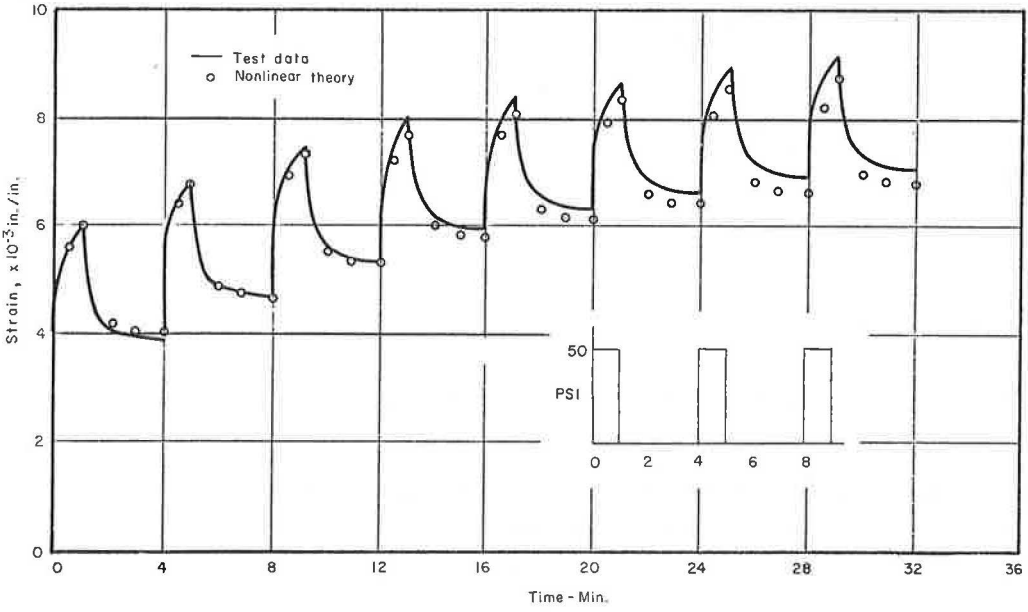

Figure 19. Results and predictions of creep behavior under cyclic loading (40-psi stress amplitude, 100 cycles).

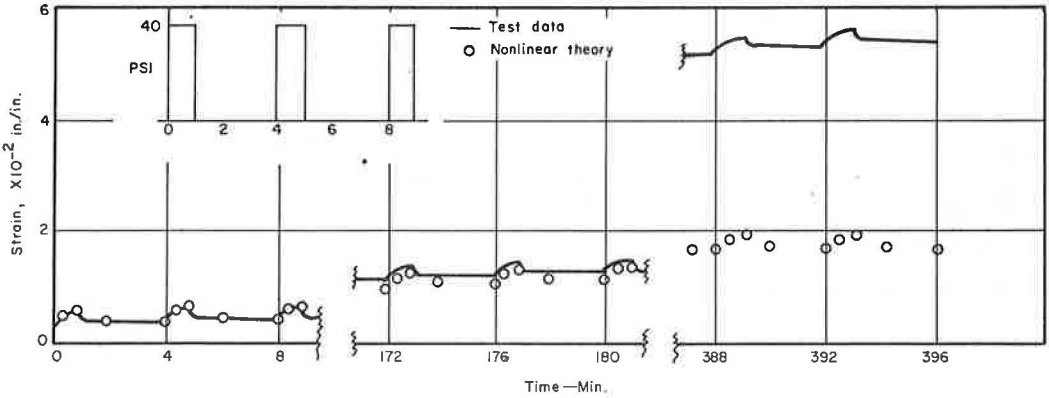

Figure 20. Irrecoverable and theoretical strains versus cycle number.

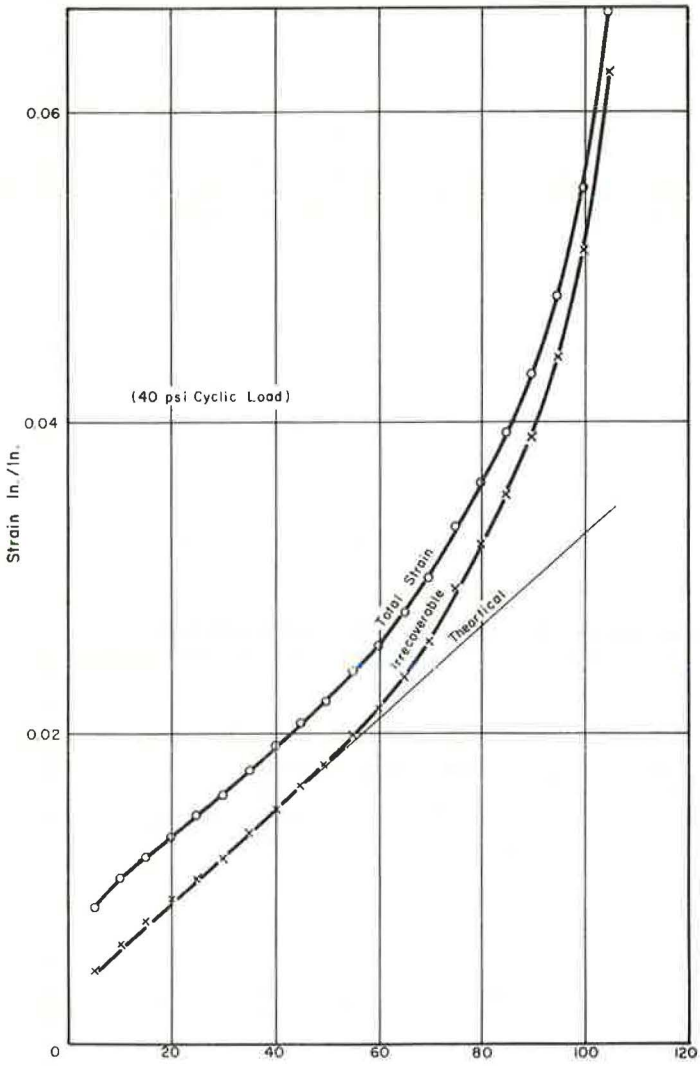

Figure 21. Irrecoverable and recoverable portions of total strain in a repeated loading test.

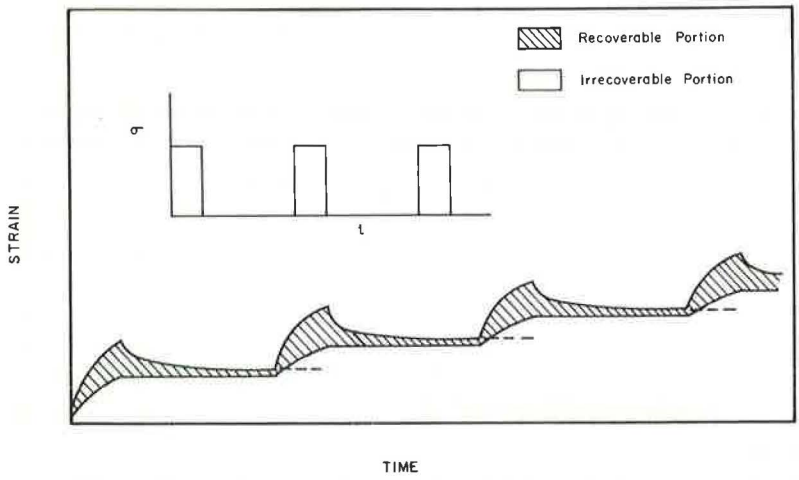

Eq. 20. Furthermore, if the maximum strain ϵ_{max} (as approximated by the $\epsilon_{p^{max}}$) is chosen to be the failure criterion of a material, Eq. 20, after rewriting into the following form, implies that

$$N = \frac{1}{(\Delta t)} \left(\frac{\epsilon_{p^{max}}}{b_1 \sigma + b_2 \sigma^2} \right)^{1/n_P} \tag{21}$$

The longer the loading time during each cycle and the larger the stress amplitude are, the fewer the number of cycles the material can withstand. Although Eq. 21 is derived from the viscoelastic characterization of asphalt concrete, some similar conclusions, such as the effect of load duration, effect of ultimate strain (tensile strain), and magnitude of stress amplitude on the fatigues life of asphalt concrete, have been reached in other fatigue studies (14, 15).

CONCLUSION

It has been shown that the nonlinear viscoelastic behavior of an asphalt concrete can be represented by a nonlinear generalized Kelvin model that is made of a nonlinear dashpot connected in series with a nonlinear Kelvin chain. The nonlinear dashpot accounts for the time-dependent irrecoverable strain (viscous flow), and the nonlinear Kelvin chain accounts for the power-law time-dependent recoverable strain. It has been shown that the constitutive equation can be determined relatively simply by utilizing both the creep and recovery parts of the constant stress creep test results. The accuracy in predicting the creep behavior of the asphalt concrete under multiple-step loading and repeated loadings using the proposed constitutive equation is very satisfactory.

It has also been shown that an equation relating the number of cycles to failure to the applied stress amplitude and the duration of each cycle similar to the existing fatigue theories can be derived from the irrecoverable creep strains. It is hoped that this study will lead to a better understanding of the time-dependent behavior of asphalt concrete.

In this report, only a single asphalt concrete mixture was utilized for the investigations, which were conducted under only one temperature (75 ±F). Though it is anticipated that varying the mixtures and the testing temperatures would definitely affect the creep behavior of asphalt concrete, some of the preliminary experimental results indicate that the difference of the creep behavior of different asphalt concrete mixtures at different temperatures (above the glass transition temperature) is more quantitative than qualitative.

REFERENCES

1. Secor, K. E., and Monismith, C. L. Analysis of Triaxial Test Data on Asphalt Concrete Using Viscoelastic Principles. HRB Proc., Vol. 40, 1961, pp. 259-314.
2. Monismith, C. L., and Secor, K. E. Viscoelastic Behavior of Asphalt Concrete Pavements. Proc. Internat. Conf. on the Structural Design of Asphalt Pavements, Univ. of Michigan, 1963.
3. Pagen, C. A. An Analysis of the Thermorheological Response of Bituminous Concrete. Ohio State Univ., PhD thesis, 1963.
4. Fitzgerald, J. E., and Lai, J. S. Initial Evaluation of the Effect of Synthetic Rubber Additives on the Thermorheological Properties of Asphalt Mixtures. Highway Research Record 313, 1970, pp. 18-31.
5. Pagazian, H. S. The Response of Linear Viscoelastic Materials in the Frequency Domain With Emphasis on Asphalt Concrete. Proc. Internat. Conf. on the Structural Design of Asphalt Pavement, Univ. of Michigan, 1962.
6. Pagen, C. A. Rheological Response of Bituminous Concrete. Highway Research Record 67, 1965, pp. 1-26.
7. Kallas, B. F., and Riley, S. C. Mechanical Properties of Asphalt Pavement Materials. Proc. Second Internat. Conf. on the Structural Design of Asphalt Pavements, Univ. of Michigan, 1967.

8. Swami, S. A., Goetz, W. H., and Harr, M. E. Time and Load Independent Properties of Bituminous Mixtures. Highway Research Record 313, 1970, pp. 63-78.
9. Findley, W. N., and Lai, J. S. A Modified Superposition Principle Applied to Creep of Nonlinear Viscoelastic Material. Trans. Soc. of Rheology, Vol. 11, No. 2, 1967, pp. 361-380.
10. Lai, J. S., and Findley, W. N. Stress Relaxation of Nonlinear Viscoelastic Material Under Uniaxial Strain. Trans. Soc. of Rheology, Vol. 12, No. 2, 1968, pp. 259-280.
11. Findley, W. N., Lai, J. S., and Onaian, K. Creep and Stress Relaxation of Non-Linear Viscoelastic Materials. To be published.
12. Pipkin, A. C., and Rogers, T. G. A Nonlinear Integral Representation for Viscoelastic Behavior. Jour. of Mechanics and Physics of Solids, Vol. 16, 1968, pp. 59-72.
13. Stafford, R. O. On Mathematical Forms for the Material Functions in Nonlinear Viscoelasticity. Jour. Mechanics and Physics of Solids, 1969, pp. 339-358.
14. Deacon, J. A. Materials Characterization—Experimental Behavior. HRB Spec. Rept. 126, 1971, pp. 150-179.
15. Finn, F. N. Factors Involved in the Design of Asphalt Pavement Surfaces. NCHRP Rept. 39, 1967, 112 pp.